

# A Brief Review on Dark Matter Annihilation Explanation for $e^\pm$ Excesses in Cosmic Ray

Xiao-Gang He<sup>1,2</sup>

<sup>1</sup>Center for High Energy Physics, Peking University, Beijing

<sup>2</sup>Department of Physics, Center for Theoretical Sciences, and LeCospa Center  
National Taiwan University, Taipei

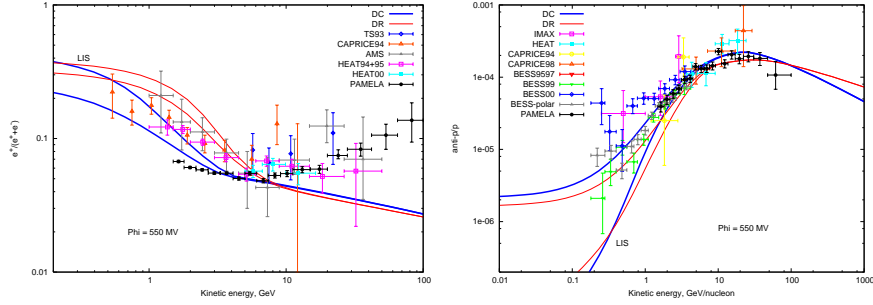
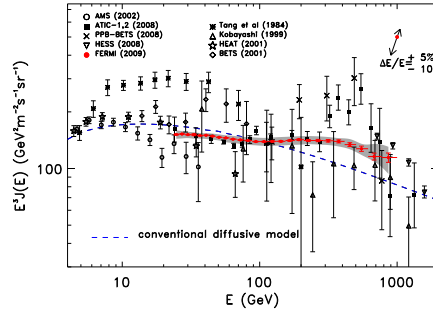
Abstract:

Recently data from PAMELA, ATIC, FERMI-LAT and HESS show that there are  $e^\pm$  excesses in the cosmic ray energy spectrum. PAMELA observed excesses only in  $e^+$ , but not in anti-proton spectrum. ATIC, FERMI-LAT and HESS observed excesses in  $e^+ + e^-$  spectrum, but the detailed shapes are different which requires future experimental observations to pin down the correct data set. Nevertheless a lot of efforts have been made to explain the observed  $e^\pm$  excesses, and also why PAMELA only observed excesses in  $e^+$  but not in anti-proton. In this brief review we discuss one of the most popular mechanisms to explain the data, the dark matter annihilation. It has long been known that about 23% of our universe is made of relic dark matter. If the relic dark matter was thermally produced, the annihilation rate is constrained resulting in the need of a large boost factor to explain the data. We will discuss in detail how a large boost factor can be obtained by the Sommerfeld and Briet-Wigner enhancement mechanisms. Some implications for particle physics model buildings will also be discussed.

*Keywords:* Dark matter,  $e^\pm$  excess, Annihilation, Boost factor, Particle

## 1. Introduction

Recently several experiments have reported  $e^\pm$  excesses in cosmic ray energy spectrum. Last year the PAMELA collaboration reported  $e^+$  excesses in the cosmic ray energy spectrum from 10 to 100 GeV, but observed no anti-proton excess [1, 2] compared with predictions from cosmic ray physics [3–6]. These results are compatible with the previous HEAT and AMS01 experiments (e.g., Ref. [7, 8]) but with higher precision. Shortly after the ATIC and PPB-BETS balloon experiments have reported excesses in the  $e^+ + e^-$  spectrum between 300 and 800 GeV [9, 10]. The ATIC data show a sharp falling in the energy spectrum around 600 GeV. Newly published result from FERMI-LAT collaboration also shows excesses in the  $e^+ + e^-$  energy spectrum above the background [11]. However, the spectrum is softer than that from ATIC. In addition, the HESS collaboration has inferred a flat but statisti-

2 *Xiao-Gang He*

 Fig. 1. Observational data and background estimate on  $e^+$  (left) and  $\bar{p}$  (right) energy spectra.

 Fig. 2. Observational data and background estimate on  $e^+ + e^-$  energy spectrum.  $J$  is the total flux of  $e^+ + e^-$ .

cally limited  $e^+ + e^-$  spectrum between 340 GeV and 1 TeV [12] which falls steeply above 1 TeV [13]. The summary of data are shown in Fig. 1 and Fig. 2 adapted from references [6] and [11].

Although astrophysics calculations of background  $e^\pm$  spectrum in our galaxy have errors due to model parameters [3–6], within reasonable ranges it is not possible to eliminate the excesses in the energy range from 10 GeV to 1 TeV. The  $e^\pm$  excesses in cosmic ray have generated much excitement in particle physics community because dark matter (DM), which contributes about 23% energy density of our universe with properties different than those of the standard model (SM) particles, can provide a nature explanation [14–24] [25] [26–30] [31–48] [49–51] [52–54] [55–78] [79–95] [96–130] [131–133] [134–137].

If the data from recent PAMELA, ATIC, FERMI-LAT and HESS are confirmed, one can extract a lot of information about dark matter. The mass of the annihilating DM serves as the cut off scale of the  $e^\pm$  spectrum, the lepton spectra must have a cut off energy at the DM mass  $m_D$ . The FERMI-LAT and HESS data would require that the DM mass to be around 1 to 2 TeV. The DM belongs to the weakly interacting massive particle (WIMP) category.

To produce large enough excesses with the annihilation mechanism, it requires modifications of the usual DM properties. This is because that for the usual DM the annihilation rate producing the  $e^\pm$  excess signal is also related to the annihilation rate producing the cosmological relic DM density. The latter requires that the thermally averaged annihilation rate  $\langle \sigma v \rangle$  to be  $3 \times 10^{-26} \text{ cm}^3 \text{ s}^{-1}$ . This annihilation rate is too small by a factor of 100 to 1000 to explain the observed excess. There is the need to boost up the spectrum with a boost factor [4–6]  $B$  of 100 to 1000.

Several mechanisms have been proposed to produce a large boost factor, including the DM substructures [134–137], non-thermal production of DM mechanism [131–133], the Sommerfeld mechanism [15] [25] [138–143], and the Breit-Wigner mechanism [15] [30] [144, 145]. There are also some other proposals [146–149]. Detailed calculations based on the N-body simulation show that the boost factor from DM substructures is generally less than [134–137]  $\sim 10$ . The reason why non-thermal production of DM in the early universe can explain  $e^\pm$  excesses is because that in this scenario the interaction rate responsible for the excesses are not directly related to the relic DM density. One basically assumes that the interaction rate is that required from the  $e^\pm$  excess data, and therefore there is no need of a boost factor. The Sommerfeld and Breit-Wigner mechanisms are more of particle physics answers to the problem which require the existence of new particles. In order for the Sommerfeld mechanism to be in effective, the new particle needs to be light to allow long range interaction between DM. The Breit-Wigner mechanism works if the annihilation of DM is through s-channel and the new particle to have a mass twice of the DM mass. This is a resonant effect.

If the DM is not stable and decay predominately into leptons on time scale longer than the age of the universe, DM decay can also provide another alternative explanation to the data [6] [96–130]. The scale of the mass then provides a natural cut-off scale  $m_D/2$  for  $e^\pm$  energy spectrum. To explain FERMI-LAT and HESS data, the DM mass is then required to be around 3 TeV. The typical life-time required to fit data is a few times of  $10^{26}$ s. This time is much longer than the life-time of the universe and will not cause other cosmological problems.

One, of course, should not exclude the possibility that there may be other explanations [150–163] One of such possibilities is that the  $e^\pm$  excess is produced by near by pulsars. Electrons in the intense rotating magnetic field that surrounds the neutron star can emit synchrotron radiation that is energetic enough to produce electron and positron pairs, but much harder to produce proton and anti-proton pairs. This provides a nice answer to why PAMELA only observed positron but not anti-proton excesses. The resulting positron spectrum can be modeled as a product of a power law and a decaying exponential with a cut-off in energy. This explains why the spectrum falls off at higher energies.

In this brief review, we will concentrate on discussions of how DM annihilation can explain  $e^\pm$  excess in cosmic ray energy spectrum. The review is arranged as the following. In Sec. II, we review propagation mechanism relating the sources of  $e^\pm$  and the detected spectrum. In Sec. III. we discuss  $e^\pm$  excesses from DM annihilation.

4 *Xiao-Gang He*

Both Sommerfeld and Briet-Wigner mechanisms for a large boost factor will be explained in some details. In Sec. IV some model building aspects of DM will be discussed. Finally in Sec. V we give our conclusions.

## 2. The cosmic $e^\pm$ spectrum and the boost factor

The detected spectrum of  $e^\pm$  on the earth are different than that of the spectrum produced at the sources. The propagation from the sources to the point of detection will distort the shape because charged particles propagate diffusively in the galaxy. Some of the main effects affecting the spectrum are the interactions with interstellar media when going through galactic turbulent magnetic field and radiation which lead to energy losses of the propagating particles, and the overall convection driven by the galactic wind and re-acceleration due to the interstellar shock waves. It is a non-trivial matter to get reliable estimate for  $e^\pm$  energy spectrum taking all effects into account. Nevertheless theoretical efforts have been made to estimate the background and DM signal. A commonly used numerical package is the GALPROP which takes into account many known astrophysics effects of our galaxy [3]. This package can provide many details for energy spectra of  $e^\pm$ , anti-proton and other particles. To have some understanding of the physics involved and also to have some simple estimate of the  $e^\pm$  spectrum, we will describe a simplified method to evaluate the  $e^\pm$  spectrum from DM annihilation in the following.

Neglecting convection and re-acceleration effects, the flux per unit energy of ultra-relativistic positron or electron is given by  $\Phi_e(t, r, E) = f(t, r, E)/4\pi$  with  $f$  obeys the diffusion equation [14]

$$\frac{\partial f}{\partial t} = K(E) \nabla^2 f + \frac{\partial(b(E)f)}{\partial E} + Q_e, \quad (1)$$

where  $K(E)$  is the diffusion coefficient which are usually parameterized as  $K_0(E/\text{GeV})^\delta$ , and  $b(E) = E^2/(\text{GeV}\tau_E)$  is the energy loss coefficient with  $\tau_E = 10^{16}\text{s}$ . These terms describe transport through the turbulent magnetic fields and energy loss due to synchrotron radiation and inverse Compton scattering on galactic photons.  $Q_e$  is the source term given by

$$Q_e(\vec{r}, E) = \frac{1}{2} \left( \frac{\rho(\vec{r})}{m_D} \right)^2 \langle \sigma v \rangle \frac{dN_e}{dE}, \quad (2)$$

where  $dN_e/dE$  is the spectrum of the electron or positron produced by DM annihilation, and  $\rho(\vec{r})$  is DM density at  $\vec{r}$ .

The above equation is then solved in a diffusive region with the shape of a solid cylinder that sandwiches the galactic plane, with height  $2L$  in the  $z$  direction and radius  $R = 20$  kpc in the  $r$  direction. The location of the solar system corresponds to  $\vec{r} = (r_{sun}; z_{sun}) = ((8.5 \pm 0.5)\text{kpc}; 0)$ . The boundary conditions are usually set to be that the  $e^+$  or  $e^-$  density vanishes on the surface of the diffusive cylinder, outside of which turbulent magnetic fields can be neglected so that positrons freely propagate and escape.

The values of the propagation parameters  $\delta$ ,  $K_0$  and  $L$  are deduced from a variety of cosmic ray data and modelizations. The following three sets of parameters have been used frequently [164]: i) *Min* :  $\delta = 0.55$ ,  $K_0 = 0.000595 \text{kpc}^2/\text{Myr}$ ,  $L = 1 \text{kpc}$ ; ii) *Med* :  $\delta = 0.70$ ,  $K_0 = 0.0112 \text{kpc}^2/\text{Myr}$ ,  $L = 4 \text{kpc}$ ; and iii) *Max* :  $\delta = 0.46$ ,  $K_0 = 0.0765 \text{kpc}^2/\text{Myr}$ ,  $L = 15 \text{kpc}$ .

To finally obtain the solution for eq.(1) one has also to know the details of the DM halo profile. There are different models. Some of the popular ones can be casted into the following form:

$$\rho(\vec{r}) = \rho_{sun} \left( \frac{r_{sun}}{r} \right)^\gamma \left( \frac{1 + (r_{sun}/r_s)^\alpha}{1 + (r/r_s)^\alpha} \right)^{(\beta-\gamma)/\alpha}, \quad (3)$$

where  $\rho_{sun}$  is the DM density at the earth position which is believed to be in the range  $0.2 \sim 0.7$  and most of the studies use 0.3. For the other parameters  $\alpha$ ,  $\beta$ ,  $\gamma$  and  $r_s$  in the profile, different values have been used. For example: a) the Core Isothermal (CI) model [165] has  $\alpha = 2$ ,  $\beta = 2$ ,  $\gamma = 0$  and  $r_s = 5 \text{kpc}$ ; b) the Navarro, Frenk and White (NFW) model [166] has  $\alpha = 1$ ,  $\beta = 3$ ,  $\gamma = 1$  and  $r_s = 20 \text{kpc}$ ; and c) the Moore model [167] has  $\alpha = 1$ ,  $\beta = 3$ ,  $\gamma = 1.16$  and  $r_s = 30 \text{kpc}$ .

For practical uses, it is convenient to factor out the galactic astrophysics modeling for the propagation and particle physics modeling of the inject spectrum  $dN_e/dE$ , and write the final flux of stationary solution of eq.(1) ( $\partial f/\partial E = 0$ ) at the detection point in the following form

$$\Phi_e(E, \vec{r}_{sun}) = B \frac{1}{4\pi b(E)} \frac{1}{2} \left( \frac{\rho_{sun}}{m_D} \right)^2 \int_E^{m_D} dE' < \sigma v > \frac{dN_e}{dE'} I_a(\lambda_D(E, E')), \quad (4)$$

where  $\lambda_D^2 = 4K_0\tau_E((E'/\text{GeV})^{\delta-1} - (E/\text{GeV})^{\delta-1})/(\delta-1)$ . The function  $I_a$  encodes the galactic astrophysics. The particle physics producing the inject positron is contained in  $dN_e/dE$ . Numerical solutions for  $I_a$  have been obtained in Ref. [14] using the CI, NFW and More models for the Min, Med and Max parameter sets. The factor  $B$  is the so called boost factor. If the model of propagation is correct, the factor  $B$  should be equal to 1. Approximate analytic forms for  $\Phi_e$  have also been obtained in the literature. For example, for the NFW profile, the annihilation flux, to a good approximation one can write  $I_a$  in the following form [14]

$$I(\lambda_D) = a_0 + a_1 \tanh \left( \frac{b_1 - l}{c_1} \right) \left( a_2 \exp \left[ -\frac{(l - b_2)^2}{c_2} \right] + a_3 \right), \quad (5)$$

where  $l = \log_{10}(\lambda_D/\text{kpc})$ .

Fitting numerical results, the following are obtained in Ref. [14]

$$\begin{aligned} \text{Min} : a &= -0.9716, b = -10.012; \\ a_0 &= 0.500, a_1 = 0.774, a_2 = -0.448, a_3 = 0.649, \\ b_1 &= 0.096, b_2 = 192.8, c_1 = 0.211, c_2 = 33.88. \end{aligned} \quad (6)$$

6 *Xiao-Gang He*

$$\begin{aligned}
 Med : a &= -1.0203, b = -1.4493 ; \\
 a_0 &= 0.502, a_1 = 0.621, a_2 = 0.688, a_3 = 0.806, \\
 b_1 &= 0.891, b_2 = 0.721, c_1 = 0.143, c_2 = 0.071.
 \end{aligned} \tag{7}$$

$$\begin{aligned}
 Max : a &= -0.9809, b = -1.1456 ; \\
 a_0 &= 0.502, a_1 = 0.756, a_2 = 1.533, a_3 = 0.672, \\
 b_1 &= 1.205, b_2 = 0.799, c_1 = 0.155, c_2 = 0.067.
 \end{aligned} \tag{8}$$

To compare with data, one has also to have knowledge about the background. The background  $e^\pm$  fluxes from astrophysical sources are believed to be mainly due to supernova explosions for the primary electrons and from the interactions between the cosmic ray nuclei, such as proton and light atoms, such as hydrogen and helium, in the interstellar medium for the secondary electrons and positrons. They are commonly parameterized in the following form [5],

$$\begin{aligned}
 \Phi_{e^-}^{bkgd,prim} &= \frac{0.16E^{-1.1}}{1 + 11E^{0.9} + 3.2E^{2.15}}, & \Phi_{e^-}^{bkgd,sec} &= \frac{0.7E^{0.7}}{1 + 110E^{1.5} + 580E^{4.2}}, \\
 \Phi_e^{bkgd,sec} &= \frac{4.5E^{0.7}}{1 + 650E^{2.3} + 15000E^{4.2}}.
 \end{aligned} \tag{9}$$

In the above the energy  $E$  is in unit GeV.

With the background  $e^\pm$  spectra known, one can say more about the role of DM in explaining the observed  $e^\pm$  excesses.

The above set of background spectra agree well with the more sophisticated numerical simulation results shown in Figs. 1 and 2 for energy larger than 10 GeV. The  $e^\pm$  excesses observed by PAMELA, ATIC, FERMI-LAT and HESS have to be due to other contributions. If DM annihilation can explain the excesses, the ratio  $\Phi_{e^+}/(\Phi_{e^+} + \Phi_{e^-})_{data}$  observed by PAMELA, and the normalized flux  $E_e^3(\Phi_{e^+} + \Phi_{e^-})_{data}$  observed by ATIC, FERMI-LAT and HESS must be equal to the background plus the DM generated fluxes,

$$\begin{aligned}
 \left( \frac{\Phi_{e^+}}{\Phi_{e^+} + \Phi_{e^-}} \right)_{data} &= \frac{\Phi_{e^+}^D + \Phi_{e^+}^{bkgd,sec}}{\Phi_{e^+}^D + \Phi_{e^+}^{bkgd,sec} + \Phi_{e^-}^D + \Phi_{e^-}^{bkgd,sec} + \kappa\Phi_{e^-}^{bkgd,prim}}, \tag{10} \\
 E_e^3(\Phi_{e^+} + \Phi_{e^-})_{data} &= E_e^3(\Phi_{e^+}^D + \Phi_{e^+}^{bkgd,sec} + \Phi_{e^-}^D + \Phi_{e^-}^{bkgd,sec} + \kappa\Phi_{e^-}^{bkgd,prim}).
 \end{aligned}$$

Note that in the above a parameter  $\kappa$  has been introduced in the equations to take care uncertainties of primary background  $e^-$  production. By adjusting  $\kappa$  one expects to make a better fit to simulation data and is usually taken to be [168, 169] 0.8. If there is no DM contribution, the data show a large  $e^\pm$  excesses. DM annihilation is one of the most interesting possibilities. If true the  $e^\pm$  excess data then determine how DM contribute to the cosmic spectrum through  $dN_e/dE$ .

For DM annihilation, the parameters involved regarding DM properties are the DM mass  $m_D$ , the annihilation rate  $\langle \sigma v \rangle$ , and the spectrum  $dN_e/dE$  from annihilation. Since the excesses go up to the TeV region,  $m_D$  must also be in the TeV

region to cover the full range of excesses. With DM mass fixed, one needs to worry about what type of final states in the DM annihilation can produce the observed  $e^\pm$  spectrum shape. This depends on the properties of DM that is responsible for  $dN_e/dE$ . Several model independent studies have been carried out [15–24] and find that the shape of the spectrum can be easily obtained by several types of annihilation final states which we will comment on later.

If one uses the annihilation rate determined from relic DM calculation to calculate the  $e^\pm$  excesses, one finds that the resulting excesses from the about propagation model calculations would be smaller by a factor of 100 to 1000. A large boost factor  $B$  is needed to explain the data. This is an important issue needs to be addressed before a consistent model can be constructed and tested further.

This problem may be due our lacking of knowledge of DM substructures in our galaxy. Detailed calculations based on the N-body simulation shows that the boost factor from DM substructures is generally less than [134–137]  $\sim 10$ . Several other mechanisms have been proposed, including DM non-thermal production mechanism [131–133] the Sommerfeld effect [15] [25] [138–143] and the Breit-Wigner resonance enhancement effect [30] [144, 145]. The non-thermal production mechanism is to detach the relic DM density from the annihilation rate producing the  $e^\pm$  excesses. The annihilation rate is taken to be a parameter to be determined by the  $e^\pm$  excess data.  $B = 1$  can produce large enough excess. On the other hand, the Sommerfeld and Breit-Wigner mechanisms start with the annihilation rate determined by relic DM density and dynamically determine the boost factor. We consider these latter two effects to be more natural. In the follow section we discuss these two mechanisms.

### 3. The Sommerfeld and Breit-Wigner enhancement factors

#### 3.1. *The Sommerfeld enhancement factor*

The Sommerfeld enhancement is a non-relativistic quantum mechanical effect [170]. Since at the epoch of relic DM got out of thermal equilibrium, the DM are non-relativistic, one can treat the problem with non-relativistic Schrodinger quantum mechanics. A large boost factor can be produced if DM interacts with a light particle.

The annihilation of DM is usually a short distance effect. Assuming that it happens at the origin of a coordinate. The annihilation cross section can be approximated by a potential of the form  $V_a \delta(\vec{r})$ . Imagining now that the DM is moving in the  $z$ -direction, the wave-function can be written up to some overall normalization factor as,  $\psi_k^0(\vec{r}) = e^{ikz}$ . It is obvious that the annihilation cross section is proportional to  $|\psi_k^0(0)|^2$  since this factor represents the DM density at the origin where the annihilation occurs. The cross section  $\sigma_0$  due to the short distance interaction can be easily obtained by the usual scattering theoretical calculations.

If in addition to the short distance interaction, there is an exchange of a massless particle between the two annihilation DMs, a long range interaction potential of the

8 *Xiao-Gang He*

form  $V_C = -\alpha/r$  between the DM will be generated. Before the annihilation happens, the  $1/r$  long range force, as is well known, will distort the DM wave-function  $\psi(\vec{r})$  and therefore modify the DM density at the origin. The cross section is then proportional to  $|\psi_k(0)|^2$  resulting in a modification factor,  $S = |\psi_k(0)|^2/|\psi_k^0(0)|^2$  and the cross section is given by  $\sigma = \sigma^0 S$ . This factor is the Sommerfeld factor.

The S factor due to a long range Coulomb like potential  $V_C(r) = -\alpha/r$  can be obtained by solving the Schrodinger equation

$$E\psi_k(\vec{r}) = \left(-\frac{1}{2\mu} \nabla^2 + V_C(r)\right)\psi_k(\vec{r}), \quad (11)$$

where  $E = k^2/2\mu > 0$ .  $\mu = m_D m_D / (m_D + m_D) = m_D/2$  is the reduced mass in the center of mass frame of the two annihilating DM.

This equation is a standard central force problem and can be solved by separation of variable in the form  $\psi_k(\vec{r}) = \sum_{l,m} A_{lm} R_l(r) Y_l^m(\theta, \phi)$  with  $Y_l^m(\theta, \phi)$  being the spherical harmonic function.  $R_l(r)$  satisfies

$$\left(\frac{1}{r^2} \frac{d}{dr} r^2 \frac{d}{dr} + k^2 - 2\mu(V_C(r) + \frac{l(l+1)}{r^2})\right) R_l(r) = 0. \quad (12)$$

To obtain an analytic solution suitable for scattering problem, let us write  $R_l(r) = r^l e^{ikr} f_l(r)$ . The function  $f_l(r)$  satisfies the confluent hypergeometric equation [171]

$$z \frac{d^2}{dz^2} f_l(z) + (2(l+1) - z) \frac{d}{dz} f_l(z) - (l+1 + in) f_l(z) = 0, \quad (13)$$

where  $z = -ikr$  and  $n = -\mu\alpha/k$ . The solution is the regular confluent function  $f_l(z) = {}_1F_1(l+1+in, 2(l+1), z)$  since at  $r=0$ , the wave function must be finite. Then

$$R_l(r) = C_l r^l e^{ikr} {}_1F_1(l+1+in, 2(l+1), -2ikr), \quad (14)$$

To determine the constant  $C_l$ , one matches the asymptotic behavior at  $r \rightarrow \infty$  of the partial wave decomposition of a plane wave scattered by a potential

$$\begin{aligned} \psi_k(r, \theta) &\rightarrow e^{ikz} + \frac{e^{ikr}}{r} \sum_0^\infty (2l+1) \frac{e^{2i\delta_l} - 1}{2ikr} P_l(\cos \theta) \\ &= \frac{1}{2ikr} \sum_0^\infty (2l+1) \left( e^{ir+2i\delta_l} - e^{-i(kr-l\pi)} \right) P_l(\cos \theta), \end{aligned} \quad (15)$$

with the behavior of  $\psi_k(r, \theta) = \sum_l C_l R_l(r) P_l(\cos \theta)$  at  $r \rightarrow \infty$

$$\begin{aligned} &\sum_l C_l \frac{e^{n\pi/2} \Gamma(2l+1)}{(2k)^l \Gamma(l+1+in)} \frac{1}{2ikr} \left( e^{i(kr-l\pi/2-n \ln(2kr)+\eta_l)} - e^{-i(kr-l\pi/2-n \ln(2kr)+\eta_l)} \right) \\ &= C_l \frac{e^{n\pi/2} \Gamma(2l+1)}{(2k)^l \Gamma(l+1+in)} e^{-i(l\pi/2+n \ln 2 - \eta_l)} \\ &\times \frac{1}{2ikr} \left( e^{i(kr-n \ln(kr)-2n \ln 2 + 2\eta_l)} - e^{-i(kr-n \ln(kr)-l\pi)} \right) P_l(\cos \theta); \end{aligned} \quad (16)$$



where  $\eta_l = \arg\Gamma(l + 1 + in)$ .

Naively it seems that, keeping  $C_l$  independent of  $r$ , it is not possible to written the asymptotic form of eq.(16) into the corresponding coefficient (the same  $l$ ) in eq. (15) because the  $\ln(kr)$  factor in the exponential. This is a well known fact which happens to the Coulomb potential scattering. The  $\ln(kr)$  needs to be kept in the exponential due to the long range interaction nature of the potential. In this case the scattering phase  $\delta_l$  is equal to  $\eta_l - n \ln 2$ , and  $C_l$  is then given by

$$C_l = \frac{1}{(2l)!} (2ik)^l \Gamma(l + 1 + in) e^{-n\pi/2} e^{i(n \ln 2 - \eta_l)}. \quad (17)$$

Note that whatever modification to the wave-function at  $r = 0$ , it only happens to the S-wave,  $l = 0$  case, since for  $l \neq 0$ ,  $R_l(r) \sim r^l e^{ikr} {}_1F_1(l + 1 + in, 2(l + 1), -2ikr)$  is zero. One immediately finds that

$$\psi_k(0) = \Gamma(1 + in) e^{-n\pi/2} e^{i(n \ln 2 - \eta_0)}. \quad (18)$$

Using the identity  $\Gamma(1 + x)\Gamma(1 - x) = x\pi / \sin(x\pi)$ , one finally obtains

$$S = \frac{|\psi_k(0)|^2}{|\psi_k^0(0)|^2} = \frac{2n\pi}{e^{2n\pi} - 1} = \frac{-\alpha\pi/v}{e^{-\alpha\pi/v} - 1}. \quad (19)$$

With the Sommerfeld factor included, the cross section is given by

$$\sigma(v)v = \sigma^0(v)v \frac{-\alpha\pi/v}{e^{-\alpha\pi/v} - 1}. \quad (20)$$

If  $\alpha$  is positive, corresponding to an attractive potential,  $S$  is an enhancement factor. While for a negative  $\alpha$ , corresponding to a repulsive potential,  $S$  is a suppression factor. Also it is velocity dependent.  $S$  plays the role of the boost factor.

For S-wave annihilation, if the DM is not close to a resonant region, the cross section is almost a constant in DM velocity. Therefore boost factor for DM annihilation resulting from the relic DM is approximately the ratio of the DM velocity  $v_r$  at the relic DM decoupling time in the early universe and the velocity  $v_p$  of DM in our galaxy halo at the present, that is  $B \sim v_r/v_p$ . The average  $v_r$  at the decoupling temperature  $T_d$  is about  $\sqrt{2T_d/m_D}$  with  $T_d/m_D \sim 1/20$  leading to  $v_r \approx 0.3$ . Model estimates show that  $v_p$  is about a few times  $10^{-4}$ . With these numbers, one can see that the Sommerfeld enhancement can easily produce the needed large boost factor.

In many practical situations, the interaction between DM is not mediated by a massless particle but a massive one, and the potential produced is a Yukawa potential  $V_Y(r) = -(\alpha/r)e^{-m_\phi r}$ . Here  $m_\phi$  is the mass of the mediating particle. One needs to solve the differential equation in eq.(15) with  $V_C(r)$  replaced by  $V_Y(r)$ . Unfortunately with  $V_Y(r)$ , it is not possible to obtain a simple analytic solution. To obtain the corresponding Sommerfeld enhancement factor, numerical calculation is needed. Fig. 3 shows the enhancement factor as a function of model parameters obtained in Ref. [25]. There are regions of parameters, resonant regions, where the enhancement factor can easily be as large as 1000.

One can understand some qualitative features without detailed numerical calculations. The Yukawa potential is not a long range interaction but one with a force

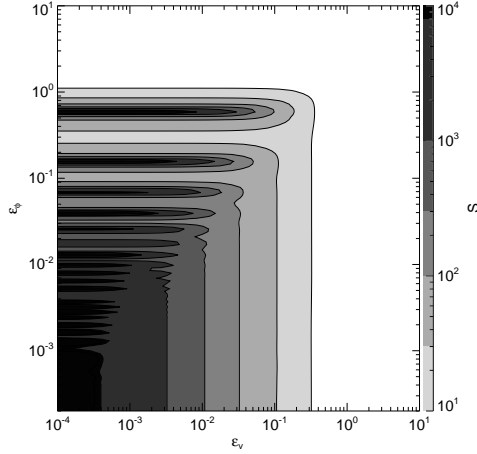


Fig. 3. The Sommerfeld factor contour as a function of  $\epsilon_v = v/\alpha$  and  $\epsilon_\phi = m_\phi/\alpha m_D$ .

range cut-off at  $r \sim 1/m_\phi$  and therefore the enhancement factor will be smaller than that due to a Coulomb potential. For  $r < 1/m_\phi$  one can expand the exponential part of the potential in power of  $r$ . Keeping the leading correction, the potential is:  $V_Y(r) \sim -(\alpha/r - \alpha m_\phi)$ . Comparing with eq.(12), one notices that if  $v^2 \gg v_s^2 = 4|\alpha|m_\phi/m_D$ , the correction term can be neglected and get back to the Coulomb potential case. At the velocity  $v_s$  the Sommerfeld enhancement starts to damp out. When the velocity slowed further down to where the corresponding deBrolie wave length  $1/m_D v_d$  of the DM to be comparable with the force range  $1/m_\phi$ , the Sommerfeld enhancement saturates itself. This sets a natural limit of the enhancement [25],  $\pi\alpha m_D/m_\phi$ .

For a detailed discussion, an more accurate form for the averaged annihilation rate should be used which can be written as [172]

$$\langle\sigma v\rangle = \frac{1}{n_{EQ}^2} \frac{m_D}{64\pi^4 x} \int_{4m_D^2}^{\infty} \hat{\sigma}(s) \sqrt{s} K_1\left(\frac{x\sqrt{s}}{m_D}\right) ds, \quad (21)$$

with

$$\begin{aligned} n_{EQ} &= \frac{g_i}{2\pi^2} \frac{m_\psi^3}{x} K_2(x), \\ \hat{\sigma}(s) &= 2g_i^2 m_\psi \sqrt{s - 4m_\psi^2} \cdot \sigma v, \end{aligned} \quad (22)$$

where  $x = m_D/T$  and  $g_i$  is the internal degrees of freedom of DM particle which is equal to 4 for a Dirac fermion.  $K_1(y)$  and  $K_2(y)$  are the modified Bessel functions of the second type.

In the non-relativistic case, the above reduces to the Maxwell-Boltzmann aver-

*A Brief Review on Dark Matter Annihilation Explanation for  $e^\pm$  Excesses in Cosmic Ray* 11

age,

$$\langle \sigma v \rangle = \int \sigma(v) v \sqrt{\frac{2}{\pi}} \frac{1}{\delta^3} v^2 e^{-v^2/2\delta^2} , \quad (23)$$

where  $\delta$  is the average DM velocity. At the relic DM decoupling, it is  $\sqrt{2T_d/m_D}$ , and at present in our galaxy halo, it is about  $10^{-4}$ .

Finally to determine the parameters one should solve the standard Boltzmann equation governing the DM abundance [172]

$$\frac{dY}{dx} = -\frac{xs(x)}{H} \langle \sigma v \rangle (Y^2 - Y_{EQ}^2) , \quad (24)$$

where  $Y = n/s(x)$  with  $n$  the DM number density and  $s(x) = 2\pi^2 g_* m_D^3 / 45x^3$  the entropy density.  $H = \sqrt{4\pi^3/45} m_D^2 / M_{PL}$  is the Hubble constant evaluated at  $x = 1$ . Here  $M_{PL} \approx 1.22 \times 10^{19}$  GeV is the Planck mass.  $g_*$  is the total relativistic degrees of freedom. In the SM  $g_* = 106.75$ . The  $Y$  value at thermal equilibrium  $Y_{EQ}$  is given by:  $(45/4\sqrt{2}\pi^{7/2})(g_i/g_*)x^{3/2}e^{-x}$ .

The rest challenge is more a particle physics one, finding a particle physics model which can have a particle  $\phi$  with small mass and interact with DM to produce the required boost factor.

### 3.2. The Breit-Wigner resonant enhancement factor

The Breit-Wigner enhancement mechanism can produce a large boost factor<sup>15,143,144</sup> if the annihilation of DM is through exchange of a particle in the S-channel with mass close to  $2m_D$ . Let us consider an example that the DM annihilates into lepton pairs by exchange of a S-channel  $Z'$ ,  $\psi\bar{\psi} \rightarrow Z' \rightarrow l\bar{l}$  through the following Lagrangian

$$L = (ag'\bar{\psi}\gamma^\mu\psi + g'\bar{l}\gamma^\mu l)Z'_\mu . \quad (25)$$

The interaction rate, to the leading order in velocity  $v$ , is given by [30]

$$\sigma(v)v = \frac{1}{\pi} \frac{a^2 g'^4 m_D^2}{(s - m_{Z'}^2)^2 + \Gamma_{Z'}^2 m_{Z'}^2} , \quad (26)$$

where  $\Gamma_{Z'}$  is the total  $Z'$  decay width and  $s$  is the center of mass frame energy squared.

If  $2m_D$  is far away from  $m_{Z'}$  the interaction rate is almost a constant. After the parameters fixed by relic DM density requirement, the interaction rate is constrained to be too small to explain the data. A large boost factor is needed. The boost factor can arise from the fact that when the  $Z'$  mass is close to  $2m_D$ , the annihilation rate is close to the resonant point. In this case the interaction rate is very sensitive to velocity of the DM. To see this let us rewrite the above annihilation rate as

$$\sigma(v)v = \frac{a^2 g'^4}{16\pi m_D^2} \frac{1}{(\delta + v^2/4)^2 + \gamma^2} , \quad (27)$$

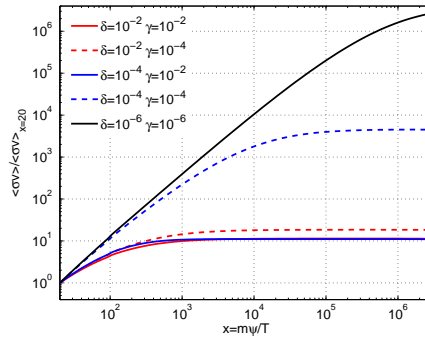


Fig. 4. The Breit-Wigner enhanced relative interaction rate  $\langle\sigma v\rangle/\langle\sigma v\rangle_{x=20}$  as a function of time  $x$ .  $m_\psi$  here is  $m_D$ .

where we have used the non-relativistic limit of  $s = 4m_D^2 + m_D^2 v^2$ , with  $\delta$  and  $\gamma$  defined as  $m_{Z'}^2 = 4m_D^2(1 - \delta)$ , and  $\gamma^2 = \Gamma_{Z'}^2(1 - \delta)/4m_D^2$ .

It is clear that for small enough  $\delta$  and  $\gamma$ , the annihilation rate is very sensitive to the velocity  $v$ . At lower velocity, the annihilation rate is enhanced. This results in a very different picture of DM annihilation than the case for the usual non-resonant annihilation where the annihilation rate is not sensitive to DM velocity. The annihilation process does not freeze out even after the usual “freeze out” time in the non-resonant annihilation case due to the enhanced annihilation rate at lower energies in the early universe. To produce the observed DM relic density, the annihilation rate at zero temperature is required to be larger than the usual one, and therefore a boost factor. With appropriate  $\delta$  and  $\gamma$ , a large enough boost factor  $B$  can be produced.

Once the interaction rate is obtained, one can use the formulae in eqs.(21) and (23) to obtain the boost factor  $B$ . A numerical evaluation obtained in Ref. [30] for the Breit-Wigner enhancement is shown in Fig. 4.

## 4. Theoretical models for dark matter

### 4.1. *Dark matter models*

Many candidate WIMP DM models have been studied in the context of the recent  $e^\pm$  data [25] [26–30] [31–48] [49–51] [52–54] [55–78] [79–95]. But not all of them can explain all the features of the  $e^\pm$  excess in cosmic ray. It turns out that the spectrum shape of the observed  $e^\pm$  excesses is easy to reproduce. For example, two body annihilation directly into  $e^\pm$  pair produces a hard spectrum which can be made consistent with ATIC data, but disfavored by FERMI-LAT and HESS data. If the two body final states are  $\mu^\pm$  or  $\tau^\pm$  pair, their subsequent decays into  $e^\pm$  can produce a soft enough spectrum consistent with FERMI-LAT and HESS data. The large boost factor and  $e^\pm$  excesses in energy spectrum but not in anti-proton

spectrum required from the data eliminate many candidate DM annihilation models. There are some doubts on the reliability of the null result for the anti-proton. But before further experimental results disprove this result, one cannot simply ignore it. In the following discussions, we will take these two as requirements for a successful model.

The simplest DM model is the Darkon model [173]. This model is the simplest in the sense that it needs the least extension from the SM. It contains in addition to the SM particles, just one real SM singlet scalar. This singlet scalar plays the role of DM. The annihilation is through exchange of the SM Higgs boson. The mass can be as large as a TeV, but should not be too small (less than a GeV) in order not to produce too large detection cross section to be ruled out by data [174, 175]. Although large boost factor can be induced if the Higgs mass is close to 2 times of the darkon mass through the Breit-Wigner enhancement mechanism, it produces too many anti-protons in the cosmic ray after fitting the  $e^\pm$  excess data. This is because that in this model the couplings of Higgs to SM fermions is proportional to fermion masses, the annihilation tends to favor heavy final states. Further extension of the model is needed to explain data.

The most popular DM candidate is the lightest supersymmetric particle (LSP) in the minimal supersymmetric standard model (MSSM). The MSSM LSP has been proposed to explain the  $e^\pm$  excesses [31–48]. However the MSSM also has problems. The LSP is a linear combination of photino, zino and higgsino. It usually has a large hadronic annihilation fraction in conflict with the PAMELA data on anti-proton cosmic ray. Also in this model there is the problem to realize a large boost factor. Gravitino DM candidate also has similar problems. Extensions are needed. There are a few papers on this subject. The next MSSM (NMSSM) model has all the right ingredients to explain the data. We will describe it more later.

In universal extra dimension (UED) models, all SM particles live in extra dimensions. After compactification of the extra dimensions, there are Kaluza-Klein (KK) excitations generated. If the size of the extra dimension  $R$  is of order  $1/TeV$ . The KK mode can play the role of DM to explain the  $e^\pm$  excesses if a discrete symmetry is applied to make KK mode stable [52–54]. The KK DM can annihilate into SM particles. For example, the  $U(1)_Y$  gauge boson KK mode can annihilate through t-channel fermion KK mode into SM fermions, and produce  $e^\pm$  excesses in cosmic ray [52–54]. However, they usually have a large hadronic fraction making the model troublesome with PAMELA anti-proton data. This problem can be remedied in the split-UED model where it is possible to split the lepton and quark KK masses such that the anti-proton cosmic ray is suppressed by larger quark KK mode masses [54]. However, these models all have problems to have a large boost factor.

Many other models [25] [26–30] [55–78] [79–95] have been proposed to explain the data. There are basically two classes of models: a) kinematically limited light particle decay models [25] [55–78]; and b) leptophilic DM models [26–30]. The light particle decay model a) requires the existence of a light particle with a mass less than the sum of proton and anti-proton masses and thus the light particle decays

predominantly into final states containing an  $e$  and/or a  $\mu$ . If final states with such a particle is the dominant annihilation channel, the  $e^\pm$  produced will be able to produce the  $e^\pm$  excesses with appropriate mechanism to acquire a large boost factor. Exchange of a light enough particle between DM can produce a large boost factor through Sommerfeld enhancement mechanism. The Breit-Wigner mechanism can also supply the boost factor. The option b), leptophilic model, can be realized by interaction of DM being leptophilic (or hadrophobic) such that interactions of the particle mediating DM annihilate only have non-zero couplings to leptons at tree level. In this case the mediating particle does not have to be light. Depending on how the annihilation occurs, it is also possible to have Sommerfeld or Breit-Wigner enhancement mechanism. In the following we discuss two models to illustrate how consistent models can be constructed.

#### 4.2. A leptophilic $Z'$ model

One of the following global symmetries in the SM can be gauged without gauge anomalies [176–180]

$$a) L_e - L_\mu, \quad b) L_e - L_\tau, \quad c) L_\mu - L_\tau .$$

At the tree-level the  $Z'$  only couples to one of the pairs  $e$  and  $\mu$ ,  $e$  and  $\tau$ , and  $\mu$  and  $\tau$ . If the  $Z'$  in one of these models is the mediating DM annihilation, the resulting final states are mainly leptonic states which can lead to excesses in  $e^\pm$  observed in cosmic rays. Of course it requires that the  $Z'$  to couple to DM [14] [27] [30]. We assume that the DM field is a fermionic field  $\psi$  with a non-trivial  $L_i - L_j$  number  $a$ . To have an anomaly free theory, this DM field should have vector-like coupling to  $Z'$ . The  $Z'$  boson can develop a finite mass  $m_{Z'}$  from spontaneous  $U(1)_{L_i - L_j}$  symmetry breaking by a non-zero vacuum expectation values  $v_s$  of a scalar  $S$  with a non-trivial charge  $L_i - L_j = b$  with  $m_{Z'}^2 = b^2 g'^2 v_s^2$ . The  $Z'$  has the desired leptophilic couplings to fermions given by [30]

$$L = -g'(a\bar{\psi}\gamma^\mu\psi + \bar{l}_i\gamma^\mu l_i - \bar{l}_j\gamma^\mu l_j + \bar{\nu}_i\gamma^\mu L\nu_i - \bar{\nu}_j\gamma^\mu L\nu_j)Z'_\mu . \quad (28)$$

The relic DM density is controlled by annihilation of  $\bar{\psi}\psi \rightarrow Z'^* \rightarrow l_i\bar{l}_i + \nu_i\bar{\nu}_i$ . The interaction rate  $\sigma v$ , with lepton masses neglected and summed over the two types of charged leptons and neutrinos, is given by

$$\sigma v = \frac{3}{\pi} \frac{a^2 g'^4 m_\psi^2}{(s - m_{Z'}^2)^2 + \Gamma_{Z'}^2 m_{Z'}^2} . \quad (29)$$

If the  $Z'$  mass is below the  $\bar{\psi}\psi$  threshold which we will assume, the dominant decay modes of  $Z'$  are  $Z' \rightarrow \bar{l}_i l_i + \bar{\nu}_i \nu_i$ , and  $\Gamma_{Z'}$  is given by, neglecting lepton masses:  $\Gamma_{Z'} = 3g'^2 m_{Z'}/12\pi$ .

In the above expressions for  $\sigma v$  and  $\Gamma_{Z'}$ , it has been assumed that there are only left-handed light neutrinos. If there are light right-handed neutrinos, the factor 3 in these equations should be changed to 4.

When calculating relic DM density, one should use the above interaction rate. However, when calculating the  $e^\pm$  spectrum, the above interaction rate needs to be multiplied by a factor of  $2/3$  since the neutrinos in the final state do not contribute to the  $e^\pm$  spectrum.

The Breit-Wigner enhancement factor can be used to generate the needed large boost factor by requiring  $m_{Z'}$  to be close to  $2m_D$ . The results obtained in Ref. [30] are shown in Fig. 5. The background is calculated using GALPROP package [3] with the diffusion + convection model parameters developed in Ref. [14]. Models a) and b), having hard  $e^\pm$  in the final state, can fit ATIC and PAMELA data [30] with DM mass 1 TeV. Model c) can fit FERMI-LAT data [30] with DM mass 1.5 to 2 TeV. Once observational data finally settled down, some of the options can be further eliminated.

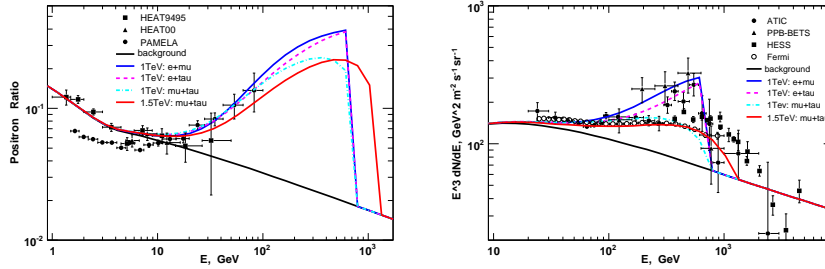


Fig. 5. *Left*: positron fraction  $e^+/(e^+ + e^-)$  predicted in the  $U(1)_{L_i-L_j}$  model compared with the observational data. *Right*: the normalized total electron spectrum of the model, compared with observational data.  $m_D = 1.5$  TeV is used in the figures.

One may also construct similar model using Sommerfeld enhancement mechanism. A possible way of achieving this is to introduce a light real scalar  $\phi$  which carries no SM quantum numbers and therefore only couples to DM in the form  $\alpha\bar{\psi}\psi\phi$ . Exchange this scalar will produce a Yukawa potential,  $V_Y(r) = -(\alpha/r)e^{-m_\phi r}$ , between DM. If the mass  $m_\phi$  is small, a few GeV, there is enough parameter space where the model can fit the data. The results are similar to the case with Breit-Wigner enhancement mechanism. The field  $\phi$  can in principle mix with the SM Higgs doublet through  $\phi$  and then decay to SM particles. If the mixing is small enough it can avoid many potential phenomenological constraints.

The main difference for models with Breit-Wigner and Sommerfeld enhancement mechanisms is that in the former model  $m_{Z'}$  is fixed to be close to  $2m_D$ , while the latter model  $m_{Z'}$  can have a much smaller mass leaving better chance for LHC study. Some of the discussions on LHC physics discussed in Ref. [27] can be applied. If there is kinetic mixing term [181]  $F^{\mu\nu}B_{\mu\nu}$  between the field strength  $B_{\mu\nu}$  of the  $U(1)_Y$  and the field strength  $F^{\mu\nu}$  of the new  $U(1)_{L_i-L_j}$ , then there is chance to have more couplings to hadron states making LHC study more relevant. This scenario is worth

further investigation.

Another interesting possibility is that the  $U(1)_{L_i-L_j}$  gauge boson  $Z'$  mass is actually very small [176–180] ( $O(\text{GeV})$ ). With the Sommerfeld mechanism provides the boost factor, the  $e^\pm$  is produced by t-channel  $\psi\bar{\psi} \rightarrow Z'Z'$  first and then  $Z'$  decays into final product with  $e^\pm$ . In this case the light  $Z'$  may be produced at low energy through [182]  $e^+e^- \rightarrow Z'\gamma$ .

### 4.3. A light particle decay model

As mentioned earlier that MSSM has problem accommodating  $e^\pm$  excesses in cosmic ray data and there is the need to extend the model to explain data. It has been shown that the NMSSM [183–186] can have all the required ingredients. The NMSSM has, in addition to the usual MSSM particle contents, a SM singlet chiral super-field  $\hat{S}$ . The fermionic partner of  $\hat{S}$  is the singlino,  $\chi$ . The spin-0 partner  $S$  contains a scalar  $h = \text{Re}(S)/\sqrt{2}$  and a pseudoscalar  $a = \text{Im}(S)/\sqrt{2}$ . The allowed renormalizable super-potential  $W_s$  and soft SUSY breaking potential  $V_s$  are given by [49, 50]

$$\begin{aligned} W_s &= v_0^2 \hat{S} + \frac{1}{2} \mu_s \hat{S}^2 + \lambda \hat{H}_u \hat{H}_d \hat{S} + \frac{1}{3} \kappa \hat{S}^3, \\ V_s &= -\left[ \frac{1}{2} m_s^2 S^\dagger S + B_s S^2 + \lambda A_\lambda H_u H_d S + \kappa A_\kappa S^3 \right] + H.C., \end{aligned} \quad (30)$$

where  $\hat{H}_{u,d}$  are the MSSM SM doublet super-fields. If a  $Z_3$  discrete symmetry is imposed on  $W_s$  and  $V_s$ , only  $m_s$ ,  $\lambda$ ,  $\kappa$ ,  $A_\lambda$  and  $A_\kappa$  are allowed.

With suitable parameters in the model the singlino  $\chi$  can have a very small mixing with other SUSY neutral fermionic fields and is the lightest super particle (LSP) playing the role of DM. The singlino mainly annihilates into the scalar  $h$  and the pseudoscalar  $a$ ,  $\chi\chi \rightarrow ah$ , through  $t$  and  $u$  channel exchanges of  $\chi$ , and s-channel exchange of  $a$ . With non-zero  $\chi\chi h$ ,  $\chi\chi a$  and  $haa$  couplings,  $T_{h\chi\chi}$ ,  $T_{a\chi\chi}$  and  $g_{haa}$ , respectively, the interaction rate is given by [49]

$$\sigma(\chi\chi \rightarrow ah)v \approx \frac{1}{64\pi m_\chi^2} \left( \frac{1}{16m_\chi^2} g_{haa}^2 T_{a\chi\chi}^2 + T_{h\chi\chi}^2 T_{a\chi\chi}^2 - \frac{1}{2m_\chi} g_{haa} T_{h\chi\chi} T_{a\chi\chi}^2 \right) \quad (31)$$

The singlino  $\chi$  can also annihilate into  $hh$  and  $aa$  final state from  $t$  and  $u$  channel  $\chi$  exchanges. But these contributions are suppressed by  $v^2$  and do not play a substantial role.

The  $h$  and  $a$  can mix with the Higgs and the pseudoscalar in the MSSM and therefore can decay into SM particles. If  $a$  has a mass  $m_a$  below the threshold of hadronization, it will not decay into proton and anti-proton pair or even pions. If  $h$  mass  $m_h$  is larger than  $2m_a$ ,  $h \rightarrow aa$  is the main decay channel for  $h$ . This way the final products of  $\chi\chi \rightarrow ah \rightarrow aaa$  have no proton and anti-proton complying with PAMELA data. If  $m_a$  is smaller than  $2m_\pi$  but larger than  $2m_\mu$ ,  $a$  predominately decays into  $\mu^+\mu^-$  pairs and then  $\mu \rightarrow \nu_\mu e \bar{\nu}_e$ . In fact there is a hint from hyperCP measurement [187] that there is a light particle of mass 214 MeV from  $\Sigma^+ \rightarrow p\mu^+\mu^-$  data and the NMSSM particle  $a$  fits that well [188]. The  $e^\pm$  excess produced this way



will have soft  $e^\pm$  spectra. It is not possible to produce a peak like spectrum in the ATIC data. But with  $\chi$  mass  $m_\chi$  of order 2 TeV, the PAMELA and FERMI-LAT spectra can be explained.

Exchange of the scalar field  $h$  between singlino  $\chi$  produces an attractive Yukawa potential  $V_Y(r) = -(\alpha/r)e^{-m_h r}$ . If  $m_h$  is light enough, less than a few GeV, a large Sommerfeld enhancement factor can be produced which then supply the much needed boost factor. This is a quit economic model. Fig. 6 shows how the PAMELA data can be fitted [49] with singlino mass of 600 GeV. But with  $\chi$  mass  $m_\chi$  of order 2TeV, although there may be the need of tuning the parameters, the PAMELA and FERMI-LAT spectra can be explained.

If the mixing of  $a$  with the MSSM heavy pseudoscalar  $A$  is significant. The annihilation rate  $\chi\chi \rightarrow A \rightarrow ah$  can be large when the mass  $m_A$  of the field  $A$  is close to  $2m_\chi$ . In this case the Breit-Wigner mechanism for the large boost factor  $B$  can be in operation, and also explain the data [51]. In this case  $m_A$  is predicted to be  $2m_D$  which would in the range for 3 to 4 TeV.

In this types of model, if the light intermediate state does couple to quarks, even it is kinematically limit to decay directly in to final states containing anti-proton or proton, there are off-shell contributions, but the rate is suppressed.

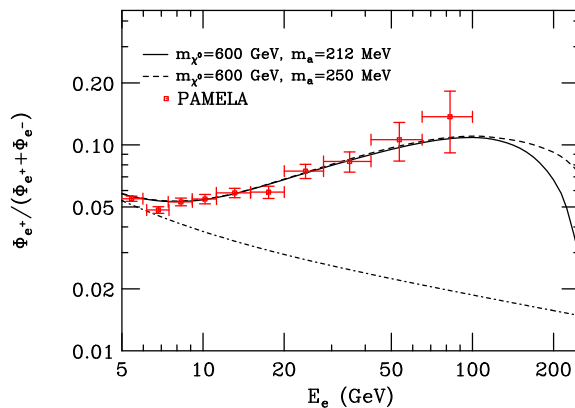


Fig. 6. The cosmic ray positron fraction resulting from singlino DM annihilations. The  $e^\pm$  spectrum is produced by  $\chi\chi \rightarrow ha$  followed by  $h \rightarrow aa$  and  $a \rightarrow \mu^+\mu^-$ .  $m_h$  is taken to be 10 GeV. The dot-dashed line denotes the prediction from astrophysical secondary production alone.

## 5. Discussions and Conclusions

In previous discussions we have concentrated on explanation of  $e^\pm$  excesses. Models constructed for this purpose have many other testable consequences. We list, without detailed discussions, some of the interesting subjects which can further reveal DM properties: a) Many of the models predict anti-proton excesses at higher energies. Measurements of anti-proton with energy beyond the PAMELA range can

reveal more details of DM b) Almost all DM annihilation models predict certain level excesses of  $\gamma$  ray. Further improved data on  $\gamma$  ray can distinguish different models. c) Some of the models proposed, such as leptophilic models, predict very small cross sections for detection, but some other models with larger values. Direct detection of DM is certainly important to distinguish models. d) In some of the models there are light new particles. Negative results of direct detection of these particles can rule out some of these models. e) High energy collider search for DM or DM annihilation mediating particles or new light particles. LHC, ILC and CLIC can also play important role in distinguish different models.

We conclude that DM annihilation can provide a consistent explanation for the recently observed  $e^\pm$  excesses in cosmic ray. In order to cover the whole energy range of excesses observed, the DM mass must be as large as the highest energy observed showing excesses. The FERMI-LAT and HESS data then require the DM to be around 1.5 to 2 TeV. To produce large enough excesses with the annihilation mechanism, it requires modifications of the usual DM properties because that the same DM annihilation process is also required to produce the relic DM density in the early universe. With this constraint, a large boost factor in the range 100 to 1000 is needed to explain data. This boost factor can be provided by particle physics effects. We have discussed two popular ones, the Sommerfeld and Breit-Wigner mechanisms. These two mechanisms have different consequences which can be distinguished by future experimental observations. The Breit-Wigner mechanism requires that the annihilation is through s-channel and the mediating particle has a mass close to two times of the DM mass. While the Sommerfeld mechanism requires the existence of a light particle of mass less than a few GeV. The PAMELA result of no anti-proton excesses further constrain how DM is annihilated. There are two classes of models, the leptophilic and the kinematically limited light particle decay models. The former requires the couplings cause the annihilation only have non-zero values for leptons, and the latter requires a new particle which the DM primarily annihilate into and this particle subsequently decays into leptons. Because this particle has a small mass which is kinematically forbidden to decay into proton or anti-proton and therefore explain the PAMELA null excess of anti-proton. All models modify what was called the usual WIMP DM. There are very different features for different types of models which can be tested. To further understand the properties of DM, more experimental observations are needed.

Acknowledgements: I thank Xiao-Jun Bi for useful discussions, and also Xiao-Jun Bi and Qiang Yuan for collaborating on related subjects. This work was supported by NSC and NCTS.

## References

1. O. Adriani *et al.* [PAMELA Collaboration], *Nature* **458**, 607 (2009).
2. O. Adriani *et al.*, *Phys. Rev. Lett.* **102**, 051101 (2009).
3. A. W. Strong and I. V. Moskalenko, [astro-ph/9906228](#); [astro-ph/0106504](#).
4. A. E. Nelson and C. Spitzer, [arXiv:0810.5167 \[hep-ph\]](#).

5. E. A. Baltz and J. Edsjo, Phys. Rev. **D59**, 023511 (1999).
6. P. f. Yin et al., Phys. Rev. D **79**, 023512 (2009).
7. S. W. Barwick *et al.* [HEAT Collaboration], Astrophys. J. **482**, L191 (1997).
8. M. Aguilar *et al.* [AMS-01 Collaboration], Phys. Lett. B **646**, 145 (2007).
9. J. Chang *et al.*, Nature **456**, 362 (2008).
10. S. Torii *et al.*, arXiv:0809.0760 [astro-ph].
11. A. A. Abdo *et al.* [The Fermi LAT Collaboration], Phys. Rev. Lett. **102**, 181101 (2009).
12. F. Aharonian et al. [H.E.S.S. Collaboration], arXiv:0905.0105 [astro-ph.HE].
13. F. Aharonian et al. [H.E.S.S. Collaboration], Phys. Rev. Lett. **101**, 261104 (2008).
14. M. Cirelli, R. Franceschini and A. Strumia, Nucl. Phys. B **800**, 204 (2008).
15. M. Cirelli, M. Kadastik, M. Raidal and A. Strumia, Nucl. Phys. B **813**, 1 (2009).
16. V. Barger, W. Y. Keung, D. Marfatia and G. Shaughnessy, Phys. Lett. B **672**, 141 (2009).
17. P. D. Serpico, Phys. Rev. D **79**, 021302 (2009).
18. C. R. Chen et al., JCAP **0905**, 015 (2009).
19. J. Mardon, Y. Nomura, D. Stolarski and J. Thaler, JCAP **0905**, 016 (2009).
20. V. Barger et al., Phys. Lett. B **678**, 283 (2009).
21. K. Cheung, P. Y. Tseng and T. C. Yuan, Phys. Lett. B **678**, 293 (2009).
22. L. Bergstrom, J. Edsjo and G. Zaharijas, arXiv:0905.0333 [astro-ph.HE].
23. P. Meade, M. Papucci, A. Strumia and T. Volansky, arXiv:0905.0480 [hep-ph].
24. J. Liu et al., arXiv:0906.3858 [astro-ph.CO].
25. N. Arkani-Hamed, D. P. Finkbeiner, T. R. Slatyer and N. Weiner, Phys. Rev. D **79**, 015014 (2009).
26. P. J. Fox and E. Poppitz, Phys. Rev. D **79**, 083528 (2009).
27. S. Baek and P. Ko, arXiv:0811.1646 [hep-ph].
28. H. S. Goh, L. J. Hall and P. Kumar, JHEP **0905**, 097 (2009).
29. H. Davoudiasl, arXiv:0904.3103 [hep-ph].
30. X. J. Bi, X. G. He and Q. Yuan, Phys. Lett. **B678**, 168 (2009).
31. L. Bergstrom, T. Bringmann and J. Edsjo, Phys. Rev. D **78**, 103520 (2008).
32. J. Hisano, M. Kawasaki, K. Kohri and K. Nakayama, Phys. Rev. D **79**, 063514 (2009).
33. K. Ishiwata, S. Matsumoto and T. Moroi, Phys. Lett. B **675**, 446 (2009).
34. J. Kalinowski, S. F. King and J. P. Roberts, JHEP **0901**, 066 (2009).
35. R. Allahverdi, B. Dutta, K. Richardson-McDaniel and Y. Santoso, Phys. Rev. D **79**, 075005 (2009).
36. P. Grajek et al., arXiv:0812.4555 [hep-ph].
37. J. H. Huh, J. E. Kim and B. Kyae, arXiv:0812.5004 [hep-ph].
38. I. Gogoladze, R. Khalid, Q. Shafi and H. Yuksel, arXiv:0901.0923 [hep-ph].
39. B. Kyae, JCAP **0907**, 028 (2009).
40. R. Allahverdi, B. Dutta, K. Richardson-McDaniel and Y. Santoso, Phys. Lett. B **677**, 172 (2009).
41. R. C. Cotta, J. S. Gainer, J. L. Hewett and T. G. Rizzo, arXiv:0903.4409 [hep-ph].
42. I. Gogoladze, R. Khalid and Q. Shafi, Phys. Rev. D **79**, 115004 (2009).
43. J. P. Hall and S. F. King, arXiv:0905.2696 [hep-ph].
44. M. Berg et al., arXiv:0906.0583 [hep-ph].
45. G. Belanger, F. Boudjema, A. Pukhov and R. K. Singh, arXiv:0906.5048 [hep-ph].
46. C. Liu, arXiv:0907.3011 [hep-ph].
47. D. Feldman, Z. Liu, P. Nath and B. D. Nelson, arXiv:0907.5392 [hep-ph].
48. D. A. Demir et al., arXiv:0906.3540 [hep-ph].
49. D. Hooper and T. M. P. Tait, arXiv:0906.0362 [hep-ph].

20 *Xiao-Gang He*

50. W. Wang, Z. Xiong, J. M. Yang and L. X. Yu, arXiv:0908.0486 [hep-ph].
51. Y. Bai, M. Carena and J. Lykken, arXiv:0905.2964 [hep-ph].
52. Y. Bai and Z. Han, Phys. Rev. D **79**, 095023 (2009).
53. D. Hooper and K. M. Zurek, Phys. Rev. D **79**, 103529 (2009).
54. C. R. Chen et al., arXiv:0903.1971 [hep-ph].
55. M. Pospelov and A. Ritz, Phys. Lett. B **671**, 391 (2009).
56. A. E. Nelson and C. Spitzer, arXiv:0810.5167 [hep-ph].
57. I. Cholis, D. P. Finkbeiner, L. Goodenough and N. Weiner, arXiv:0810.5344 [astro-ph].
58. Y. Nomura and J. Thaler, Phys. Rev. D **79**, 075008 (2009).
59. D. Feldman, Z. Liu and P. Nath, Phys. Rev. D **79**, 063509 (2009).
60. C. R. Chen, F. Takahashi and T. T. Yanagida, Phys. Lett. B **673**, 255 (2009).
61. T. Hur, H. S. Lee and C. Luhn, JHEP **0901**, 081 (2009).
62. M. Pospelov, arXiv:0811.1030 [hep-ph].
63. I. Cholis et al., arXiv:0811.3641 [astro-ph].
64. L. Bergstrom et al., Phys. Rev. D **79**, 081303 (2009).
65. E. J. Chun and J. C. Park, JCAP **0902**, 026 (2009).
66. K. Hamaguchi, S. Shirai and T. T. Yanagida, Phys. Lett. B **673**, 247 (2009).
67. K. J. Bae et al., Nucl. Phys. B **817**, 58 (2009).
68. T. Gehrman, N. Greiner and P. Schwaller, arXiv:0812.4240 [hep-ph].
69. L. Covi and J. E. Kim, arXiv:0902.0769 [astro-ph.CO].
70. R. Barbieri, L. J. Hall, V. S. Rychkov and A. Strumia, arXiv:0902.2145 [hep-ph].
71. M. Ibe, Y. Nakayama, H. Murayama and T. T. Yanagida, JHEP **0904**, 087 (2009).
72. C. Cheung, J. T. Ruderman, L. T. Wang and I. Yavin, arXiv:0902.3246 [hep-ph].
73. S. Cassel, D. M. Ghilencea and G. G. Ross, arXiv:0903.1118 [hep-ph].
74. R. Essig, P. Schuster and N. Toro, arXiv:0903.3941 [hep-ph].
75. K. Kohri, J. McDonald and N. Sahu, arXiv:0905.1312 [hep-ph].
76. S. Shirai, F. Takahashi and T. T. Yanagida, arXiv:0905.3235 [hep-ph].
77. J. Mardon, Y. Nomura and J. Thaler, arXiv:0905.3749 [hep-ph].
78. D. E. Morrissey, D. Poland and K. M. Zurek, JHEP **0907**, 050 (2009).
79. M. Cirelli, A. Strumia and M. Tamburini, Nucl. Phys. **787**, 152 (2007).
80. E. Ponton and L. Randall, JHEP **0904**, 080 (2009).
81. K. M. Zurek, Phys. Rev. D **79**, 115002 (2009).
82. X. J. Bi, P. H. Gu, T. Li and X. Zhang, JHEP **0904**, 103 (2009).
83. S. Khalil, H. S. Lee and E. Ma, Phys. Rev. D **79**, 041701R (2009).
84. Q. H. Cao, E. Ma and G. Shaughnessy, Phys. Lett. B **673**, 152 (2009).
85. E. Nezri, M. H. G. Tytgat and G. Vertongen, JCAP **0904**, 014 (2009).
86. D. J. Phalen, A. Pierce and N. Weiner, arXiv:0901.3165 [hep-ph].
87. F. Chen, J. M. Cline and A. R. Frey, Phys. Rev. D **79**, 063530 (2009).
88. P. H. Frampton and P. Q. Hung, Phys. Lett. B **675**, 411 (2009).
89. M. Cirelli and A. Strumia, arXiv:0903.3381 [hep-ph].
90. A. A. El-Zant, S. Khalil and H. Okada, arXiv:0903.5083 [hep-ph].
91. J. H. Huh, J. E. Kim and B. Kyae, arXiv:0904.1108 [hep-ph].
92. I. Gogoladze, N. Okada and Q. Shafi, arXiv:0904.2201 [hep-ph].
93. W. L. Guo and X. Zhang, Phys. Rev. D **79**, 115023 (2009).
94. X. Calmet and S. K. Majee, arXiv:0905.0956 [hep-ph].
95. P. H. Gu, H. J. He, U. Sarkar and X. m. Zhang, arXiv:0906.0442 [hep-ph].
96. C. R. Chen, F. Takahashi and T. T. Yanagida, Phys. Lett. B **671**, 71 (2009).
97. C. R. Chen and F. Takahashi, JCAP **0902**, 004 (2009).
98. K. Hamaguchi, E. Nakamura, S. Shirai and T. T. Yanagida, Phys. Lett. B **674**, 299 (2009).

99. A. Ibarra and D. Tran, *JCAP* **0902**, 021 (2009).
100. C. R. Chen, M. M. Nojiri, F. Takahashi and T. T. Yanagida, arXiv:0811.3357 [astro-ph].
101. E. Nardi, F. Sannino and A. Strumia, *JCAP* **0901**, 043 (2009).
102. K. Ishiwata, S. Matsumoto and T. Moroi, *Phys. Rev. D* **79**, 043527 (2009).
103. M. Pospelov and M. Trott, *JHEP* **0904**, 044 (2009).
104. J. Hisano, M. Kawasaki, K. Kohri and K. Nakayama, *Phys. Rev. D* **79**, 043516 (2009).
105. J. Liu, P. f. Yin and S. h. Zhu, arXiv:0812.0964 [astro-ph].
106. F. Takahashi and E. Komatsu, arXiv:0901.1915 [astro-ph].
107. C. H. Chen, C. Q. Geng and D. V. Zhuridov, arXiv:0901.2681 [hep-ph].
108. K. Hamaguchi, F. Takahashi and T. T. Yanagida, *Phys. Lett. B* **677**, 59 (2009).
109. X. Chen, arXiv:0902.0008 [hep-ph].
110. K. J. Bae and B. Kyae, *JHEP* **0905**, 102 (2009).
111. R. Essig, N. Sehgal and L. E. Strigari, *Phys. Rev. D* **80**, 023506 (2009).
112. S. Shirai, F. Takahashi and T. T. Yanagida, arXiv:0902.4770 [hep-ph].
113. K. Ishiwata, S. Matsumoto and T. Moroi, *JHEP* **0905**, 110 (2009).
114. M. Endo and T. Shindou, arXiv:0903.1813 [hep-ph].
115. S. L. Chen, R. N. Mohapatra, S. Nussinov and Y. Zhang, *Phys. Lett. B* **677**, 311 (2009).
116. K. Ishiwata, S. Matsumoto and T. Moroi, arXiv:0903.3125 [hep-ph].
117. A. Ibarra, A. Ringwald, D. Tran and C. Weniger, arXiv:0903.3625 [hep-ph].
118. A. Arvanitaki et al., arXiv:0904.2789 [hep-ph].
119. S. Shirai, F. Takahashi and T. T. Yanagida, arXiv:0905.0388 [hep-ph].
120. C. H. Chen, C. Q. Geng and D. V. Zhuridov, arXiv:0905.0652 [hep-ph].
121. N. Okada and T. Yamada, arXiv:0905.2801 [hep-ph].
122. H. Fukuoka, J. Kubo and D. Suematsu, *Phys. Lett. B* **678**, 401 (2009).
123. C. H. Chen, arXiv:0905.3425 [hep-ph].
124. L. Zhang, G. Sigl and J. Redondo, arXiv:0905.4952 [astro-ph.GA].
125. C. H. I. Chen, C. Q. I. Geng and D. V. Zhuridov, arXiv:0906.1646 [hep-ph].
126. D. Aristizabal Sierra, D. Restrepo and O. Zapata, arXiv:0907.0682 [hep-ph].
127. J. H. Huh and J. E. Kim, arXiv:0908.0152 [hep-ph].
128. D. G. E. Walker, arXiv:0907.3142 [hep-ph].
129. H. Murayama and J. Shu, arXiv:0905.1720 [hep-ph].
130. W. Buchmuller et al., arXiv:0906.1187 [hep-ph].
131. B. Dutta, L. Leblond and K. Sinha, arXiv:0904.3773 [hep-ph].
132. X. J. Bi et al., arXiv:0905.1253 [hep-ph].
133. G. Kane, R. Lu and S. Watson, arXiv:0906.4765 [astro-ph.HE].
134. J. Lavalle, Q. Yuan, D. Maurin and X. J. Bi, *Astron. Astrophys.* **479**, 427 (2008).
135. J. Lavalle et al., *Phys. Rev. D* **78**, 103526 (2008).
136. P. J. Elahi, L. M. Widrow and R. J. Thacker, arXiv:0906.4352 [astro-ph.HE].
137. Q. Yuan et al., arXiv:0905.2736 [astro-ph.HE].
138. J. Hisano, S. Matsumoto and M. M. Nojiri, *Phys. Rev. Lett.* **92**, 031303 (2004).
139. J. Hisano, S. Matsumoto, M. M. Nojiri and O. Saito, *Phys. Rev. D* **71**, 063528 (2005).
140. J. Hisano et al., *Phys. Lett. B* **646**, 34 (2007).
141. J. March-Russell, S. West D. Cumberbatch and D. Hooper, *JHEP* 0807:058 (2008).
142. M. Lattanzi and J. I. Silk, arXiv:0812.0360 [astro-ph].
143. J. Bovy, arXiv:0903.0413 [astro-ph.HE].
144. M. Ibe, H. Murayama and T. T. Yanagida, *Phys. Rev. D* **79**, 095009 (2009).
145. W. L. Guo and Y. L. Wu, *Phys. Rev. D* **79**, 055012 (2009).
146. J. D. March-Russell and S. M. West, *Phys. Lett. B* **676**, 133 (2009).

147. W. Shepherd, T. M. P. Tait and G. Zaharijas, arXiv:0901.2125 [hep-ph].
148. B. Robertson and A. Zentner, arXiv:0902.0362 [astro-ph.CO].
149. J. McDonald, arXiv:0904.0969 [hep-ph].
150. A. A. Andrianov, D. Espriu, P. Giacconi and R. Soldati, arXiv:0907.3709 [hep-ph].
151. D. Hooper, P. Blasi and P. D. Serpico, JCAP **0901**, 025 (2009).
152. J. Zhang et al., arXiv:0812.0522 [astro-ph].
153. M. Pohl, Phys. Rev. D **79**, 041301 (2009).
154. S. Profumo, arXiv:0812.4457 [astro-ph].
155. H.-B. Hu et al., APJ 700, L170(2009).
156. N. J. Shaviv, E. Nakar and T. Piran, arXiv:0902.0376 [astro-ph.HE].
157. T. Piran, N. J. Shaviv and E. Nakar, arXiv:0905.0904 [astro-ph.HE].
158. D. Malyshev, I. Cholis and J. Gelfand, arXiv:0903.1310 [astro-ph.HE].
159. P. Blasi, arXiv:0903.2794 [astro-ph.HE].
160. P. L. Biermann et al., arXiv:0903.4048 [astro-ph.HE].
161. Y. Fujita, K. Kohri, R. Yamazaki and K. Ioka, arXiv:0903.5298 [astro-ph.HE].
162. D. Grasso *et al.* [FERMI-LAT Collaboration], arXiv:0905.0636 [astro-ph.HE].
163. L. Stawarz, V. Petrosian and R. D. Blandford, arXiv:0908.1094 [astro-ph.GA].
164. T. Delahaye et al., Phys. Rev. D **77**, 063527 (2008).
165. J. N. Bahcall and R. M. Soneira, Astrophys. J. Suppl. **44**, 73 (1980).
166. J. F. Navarro, C. S. Frenk and S. D. M. White, Astrophys. J. **462**, 563(1996).
167. B. Moore et al., Mon. Not. Roy. Astron. Soc. **310**, 1147(1999).
168. I. Moskalenko and A. Strong, Astrophys. J. **493**, 694 (1998).
169. E. A. Baltz et al., Phys. Rev. **D65**, 063511 (2002).
170. A. Sommerfeld, Annalen der Physik 403, 257 (1931).
171. L.D. Landau, Quantum Mechanics: Non-Relativistic Theory, Volume 3, Third Edition (Elsevier Science Ltd).
172. P. Gondolo and G. Gelmini, Nucl. Phys. **B360**, 145 (1991).
173. V. Silveira and A. Zee, Phys. Lett. **B161**, 136 (1985).
174. X.G. He, T. Li, X.Q. Li, and H.C. Tsai, Mod. Phys. Lett.**A22**, 2121 (2007).
175. X. G. He et al., Phys. Rev. D **79**, 023521 (2009).
176. X. G. He, G. C. Joshi, H. Lew and R. R. Volkas, Phys. Rev. D **43** (1991) 22.
177. X. G. He, G. C. Joshi, H. Lew and R. R. Volkas, Phys. Rev. D **44** (1991) 2118.
178. R. Foot, X. G. He, H. Lew and R. R. Volkas, Phys. Rev. D **50** (1994) 4571.
179. S. Baek, N. G. Deshpande, X. G. He and P. Ko, Phys. Rev. D **64** (2001) 055006.
180. E. Ma, D. P. Roy and S. Roy, Phys. Lett. B **525**, 101 (2002).
181. R. Foot and X. G. He, Phys. Lett. B **267** (1991) 509.
182. P. f. Yin, J. Liu and S. h. Zhu, arXiv:0904.4644 [hep-ph].
183. H.P. Nilles, M. Srednicki, and D. Wyler, Phys. Lett. **B120**, 346 (1983).
184. J.M. Frere, D.R.T. Jones, and S. Raby, Nucl. Phys. **B222**, 11 (1983).
185. J.P. Derendinger and C.A. Savoy, *ibid.* **237**, 307 (1984).
186. J. R. Ellis et al., Phys. Rev. **D39**, 844 (1989).
187. H. Park et al. [HyperCP Collaboration], Phys. Rev. Lett. **94**, 021801 (2005).
188. X. G. He, J. Tandean and G. Valencia, Phys. Rev. Lett. **98**, 081802 (2007).